Supplement Material

Supplemental Methods, Figures, and Figure Legends

Detailed Methods

Mice. C57BL/6J mice were purchased from Jackson Laboratories. *Pai1*$^{-/-}$ mice and *Vn*$^{-/-}$ mice (backcrossed >20 generations into the C57BL/6J genetic background) were described previously.[1, 2] C57BL/6J-congenic PAI-1-transgenic (Tg) mice that over-express murine PAI-1 under the control of the CMV promoter were from Dr. David Ginsburg, University of Michigan.[3] To determine transgene copy number, we performed real-time, quantitative PCR analyses of genomic DNA isolated from PAI-1-Tg and wild-type mice, using oligonucleotide primers (5'-GTTCTGGTCTCTGGGAAAGG-3' and 5'-GCTGAAACACTTTTACTCCGAAG-3') located within exon 2 of the murine PAI-1 gene, CYBR Green I dye (BIO-RAD), and the comparative cycle threshold ($2^{-[delta][delta]Ct}$) method.[4] Our data (not shown) suggested that the PAI-1 transgene copy number of the line of PAI-1-Tg mice used in our experiments was two. To assess for the possibility that integration of the transgene disrupted function of an endogenous gene that regulates intimal hyperplasia, we compared VG intimal hyperplasia in mice homozygous (n=5) vs. heterozygous (n=7) for the PAI-1 transgene (transgene zygosity was determined by quantitative real-time PCR).[5] We observed no significant differences between transgene-homozygous and transgene-heterozygous mice (data not shown), suggesting that transgene integration did not disrupt function of an endogenous gene

that regulates VG intimal hyperplasia. All animal care and experimental procedures were approved by the University of Missouri Animal Care and Use Committee. Mice received normal chow (5008/LabDiet) before and after surgery. All surgical procedures and histological analyses were performed with the investigator blinded to mouse genotype.

Morphometric analyses. Four weeks after surgery the VG was surgically exposed. The vasculature was perfused with phosphate-buffered saline (PBS) and 4% phosphate-buffered paraformaldehyde for 2 and 5 minutes, respectively, which were injected into the left ventricle and exited the circulation through a laceration created in the liver. The VG was embedded in paraffin. Three evenly spaced cross-sections (5 μm thick, 70 μm between sections) from its mid-portion were prepared, mounted, and stained with hematoxylin and eosin. Microscopic images were imported into Image-Pro Plus (Media Cybernetics) and lumen-vascular wall and tunica media-adventitia interfaces were traced. Intima area was defined as the difference between the two traced cross-sectional areas.[6] Lumen area (A) was calculated from the length of the lumen-vascular wall interface (p), using the formula $A=p^2/4\pi$. Mean intimal area/lumen area was calculated for each VG. To measure intima thickness, the thinnest portion of the intima was designated the 12 o'clock position. Intima thickness was measured at 1:30, 3, 4:30, 6, 7:30, 9, 10:30, and 12 o'clock. Mean intima thickness was calculated for each cross-section and VG.

Immunohistochemistry. Cross-sections obtained from the mid-portions of VGs were mounted on slides, de-paraffinized, hydrated, incubated 10 minutes in 3% H_2O_2 in methanol, and rinsed with PBS. Antigens of interest were detected using the Histomouse-MAX Kit (Invitrogen) and appropriate primary and secondary antibodies. Negative control reactions lacking primary antibody confirmed the specificity of each secondary antibody. Identical, simultaneously performed immunostaining techniques (i.e. antibody dilutions, incubation and wash times) were used for all samples. PAI-1 immunostaining was performed using rabbit anti-mouse PAI-1 polyclonal antibody (Santa Cruz Biotechnology) and peroxidase-conjugated anti-rabbit-IgG. Control Western blotting experiments performed with anti-PAI-1 antibody confirmed its capacity to detect purified murine PAI-1 in concentrations as low as 10 ng/gel lane, very low non-specific immunoreactivity with antigens present in detergent extracts prepared from murine inferior vena cava (IVC), and the lack of any apparent differences in non-specific immunoreactivity between wild-type, PAI-1-deficient, and PAI-1-trangsenic IVC (data not shown). To quantify PAI-1 immunostaining, images of cross-sections were captured under identical imaging conditions and imported into Image-Pro Plus software (MediaCybernetics). Four regions of interest (ROI) were drawn at the 12, 3, 6, and 9 o'clock positions within the neointima of each VG. The amount of positive immunostaining within each ROI (expressed as positive pixels/mm^2) was determined by false color segmentation analysis, [7] using PAI-1-positive threshold settings determined from a $WT^{graft}/WT^{recipient}$ sample. Mean values of the ROIs were calculated for each VG. Mean immunostaining intensity observed in PAI-1-deficient samples (i.e. $Pai1^{-/-graft}/Pai1^{-/-recipient}$ mice, n=3) was defined as background immunostaining, and this value was

subtracted from mean observed immunostaining intensity in each VG to calculate PAI-1 immunostaining. Specificity of anti-PAI-1 antibody was demonstrated by the observed lack of significant staining in PAI-1-deficient VG, and the marked inhibition of immunostaining of PAI-1-expressing VG after preincubation of antibody with recombinant murine PAI-1 (Molecular Innovations, Supplemental Fig. IA) Fibrinogen/fibrin immunostaining was performed using goat anti-mouse fibrinogen polyclonal primary antibody (Nordic Immunology) and Texas-Red-conjugated rabbit-anti-goat-IgG antibody (Vector). Specificity of anti-fibrinogen/fibrin antibody was demonstrated by the observed lack of immunostaining in liver tissue of fibrinogen-deficient mice (provided by J. Degen, PhD, Children's Hospital Research Foundation, University of Cincinnati, Supplemental Fig. IB). Immunostaining of macrophages was performed with rat anti-Mac-3 IgG (BD Pharmingen) and Texas-Red-conjugated goat-anti-rat IgG antibody (Vector). Smooth muscle alpha-actin (SMAA) and proliferating cell nuclear antigen (PCNA) were detected with mouse-anti-human-SMAA and mouse-anti-rat-PCNA monoclonal antibodies (Santa Cruz Biotechnology) and peroxidase-conjugated anti-mouse-IgG (Invitrogen*). Q*uantification of immunostaining of specific cell types and fibrinogen was performed as described.[8]

Measurement of plasma PAI-1. Blood was collected into citrate anticoagulant by cardiac puncture. Platelet-poor plasma was prepared by centrifugation. Plasma PAI-1 concentration was determined by a conventional sandwich assay with a Luminex 100 System (Luminex Austin, TX). Murine anti-rodent PAI-1 monoclonal antibody H34G6 (Molecular Innovations, Novi, MI) linked to carboxylated microspheres was used to

capture total PAI- antigen. Human urokinase (Molecular Innovations) linked to carboxylated microspheres was used to capture active PAI-1. To detect microsphere-bound active and total PAI-1 antigen, biotinylated rabbit anti-mouse PAI-1 (Molecular Innovations) was used followed by streptavidin-R-phycoerythrin (S-866, Molecular Probes). The concentrations of active and total PAI-1 in each sample were calculated against standard curves for active and total murine PAI-1 generated from purified active murine PAI-1 (MPAI, Molecular Innovations). Lower limits of PAI-1 detection were 3.2 pg/mL and 16 pg/mL for the antigen and activity assays, respectively. Values less than these are reported as undetectable.

Reverse-transcriptase polymerase chain reaction (RT-PCR) analysis of PAI-1 gene expression. Veins were retrieved from adult mice immediately after euthanasia and rinsed extensively. Total cellular RNA was extracted using the Recover All Total Nucleic Acid Isolation Kit (Ambion). Reverse-transcriptase real-time polymerase chain reaction (RT-PCR) was performed using the High-Capacity cDNA Reverse Transcription Kit (Applied Biosystems), oligonucleotide primers specific for PAI-1 cDNA (5'-GCTGCAGATGACCACAGCGGG-3' and 5'-CCGCAGTACTGATCTCATTC-3'), and a Bio-Rad iQ5 real-time PCR detection system. Beta actin gene expression was simultaneously assessed in all samples as an internal control. Relative PAI-1 gene expression was determined by the $2^{-\Delta\Delta C}$T method.[9]

Isolation and functional assessment of venous SMC. Lines of cultured venous SMC, each originating from the IVC of a single mouse, were established by digesting veins

with collagenase (Worthington) after carefully removing loose adventitia, as described.[10] At least 3 independent lines of cells of each genotype were studied in each set of experiments. Venous SMC were grown in culture under standard conditions in DMEM/F12 medium supplemented with 20% fetal bovine serum (FBS). Cells were passaged a maximum of 7 times before being used in experiments. To study thrombin-induced proliferation, venous SMC (1.0×10^4) were seeded in 96-well plates in DMEM/F12 containing 20% FBS, glucose, Fungizone (Sigma), and gentamycin. After 3 days of standard cell culture conditions cells were washed and incubated 3 days in serum-free DMEM/F12 containing insulin-transferrin-selenium-A supplement (GibcoBRL). Alpha-thrombin (Enzyme Research Laboratories, 1 U/mL) or vehicle control was added to cells. Two days later BrdU (10 μM) was added. Eighteen hours later rates of cell proliferation were measured using the Cell Proliferation ELISA, BrdU (colorimetric) Kit (Roche), according to manufacturer's instructions. Results are reported as % of vehicle-control-treated cells. To study SMC migration, 3-dimensional rat type 1 collagen gels were prepared as described previously.[11] Polymerizing collagen mixture (30 μL) was pipetted into the upper chambers of 24-well Transwell inserts (Corning) whose bottoms consisted of porous (8 μm pore diameter) membranes. After gels polymerized, DMEM medium (200 μL) containing 0.2% FBS and SMC ($1.0x10^5$) were added to the upper chamber. Inserts were placed into lower chamber wells filled with DMEM (600 μL) containing 2.5% FBS and PDGF-BB (Upstate, 20 ng/mL), which stimulates SMC migration through the collagen gel. After 72 hr of standard cell culture conditions, inserts were removed, collagen gels were scraped away, and membranes were stained with Diff-Quick (Siemens Healthcare Diagnostics). The lower-chamber

side of the membrane, to which cells that migrated through the collagen gel and pores adhere, was visualized en-face with a microscope and cells were counted.

Statistical Analyses. Results are expressed as mean ± one standard error of the mean. One way analysis of variance with multiple comparison procedures (Holm-Sidak method) and the Students t test were used, as appropriate, to compare differences between groups. A probability (P) value of <0.05 was considered statistically significant.

Supplemental Figures and Legends

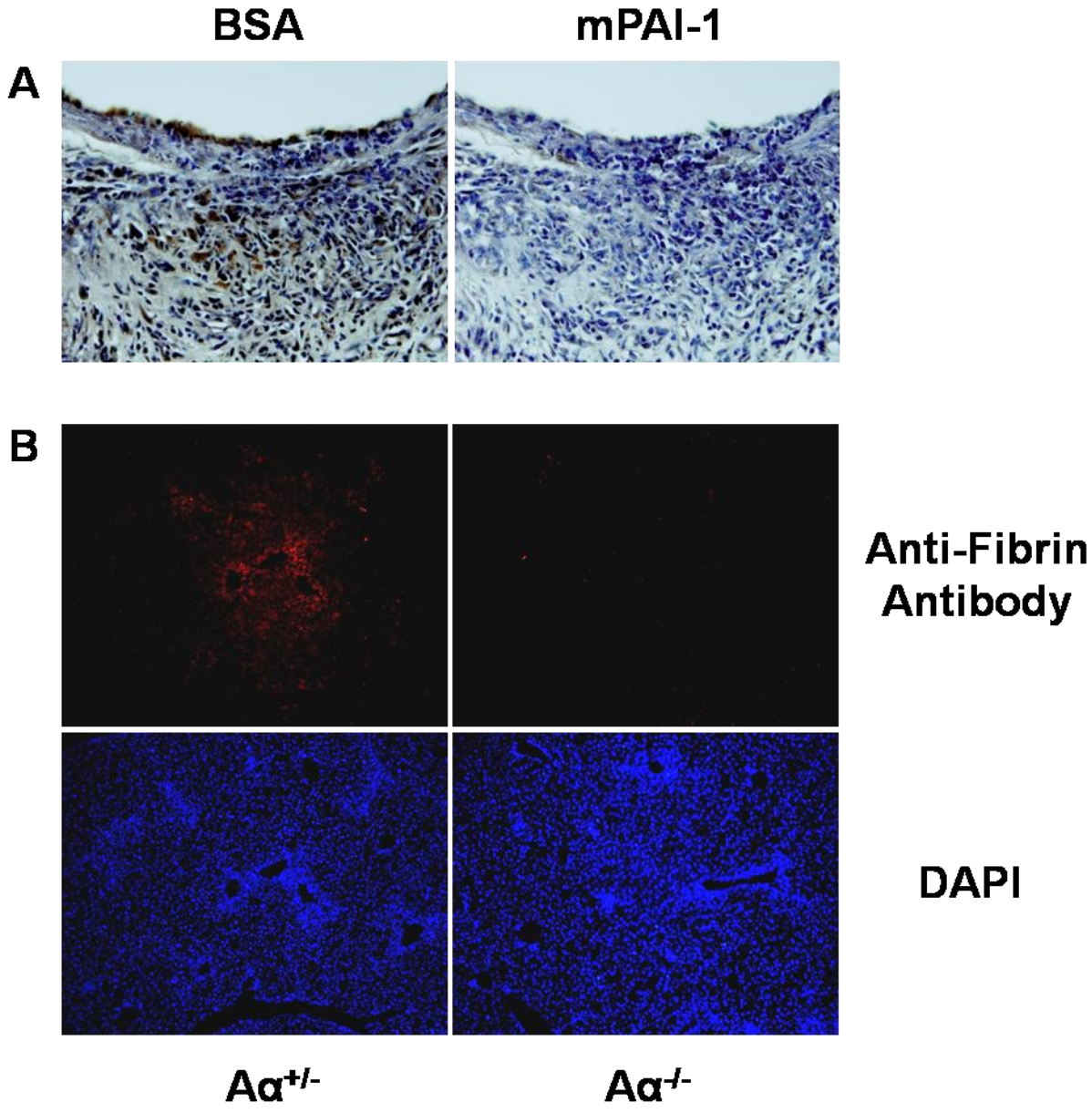

Supplemental Figure I. Characterization of specificity of antibodies. (A) Anti-PAI-1 immunostaining. Consecutive cross-sections (5 μm thickness) of a PAI-1-transgenic vein graft were immunostained with anti-PAI-1 antibody as described in Methods. For

one sample (left panel) the anti-PAI-1 antibody was pre-incubated with bovine serum albumin (10 µg/mL) prior to immunostaining. For the other sample (right panel) the anti-PAI-1 antibody was pre-incubated with recombinant murine PAI-1 (10 µg/mL, Molecular Innovations) prior to immunostaining. Note depletion of immunostaining by exposure of anti-PAI-1 antibody to soluble PAI-1. Distance bar denotes 50 µm. (B) Anti-fibrin/fibrinogen immunostaining. Liver tissue from mice exposed to carbon tetrachloride (which induces centrilobular necrosis and fibrin deposition) was generously provided by J. Degen, PhD, Children's Hospital Research Foundation, University of Cincinnati.[12, 13] Samples were immunostained with anti-fibrin antibody (upper row) or 4',6-diamidino-2-phenylindole (DAPI, a nuclear stain; lower row). Left column is liver from a fibrinogen-expressing ($A\alpha^{+/-}$) mouse. Right column is liver from a fibrinogen-null ($A\alpha^{-/-}$) mouse. Distance bar denotes 200 µm.

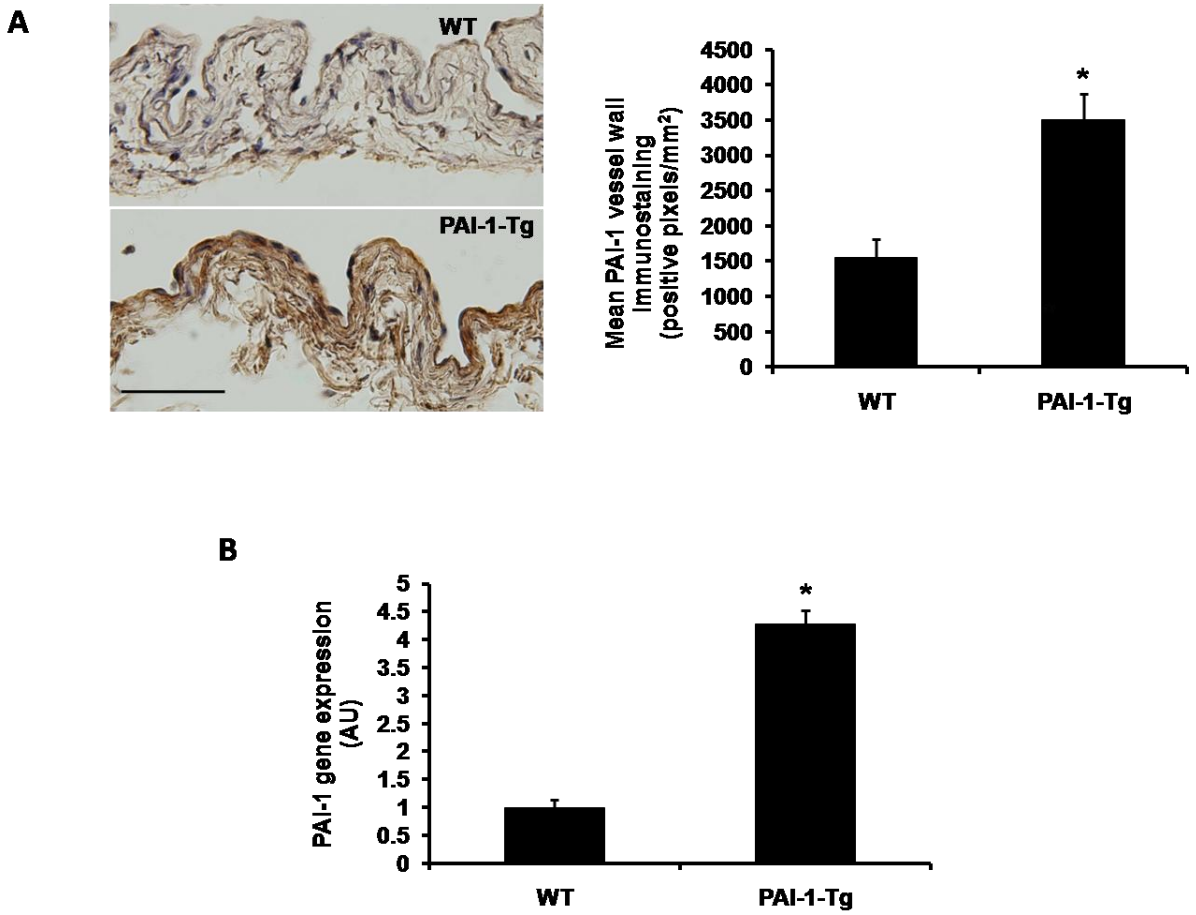

Supplemental Figure II. Analysis of PAI-1 expression in inferior vena cava (IVC) of wild-type (WT) and transgenic (PAI-1-Tg) adult mice. (A) Representative images and quantitative analysis of PAI-1 immunostaining (n=3 mice/group). *P<0.05. Distance bar represents 50 µm. (B) Real-time RT-PCR analysis of total cellular RNA isolated from IVC. AU, arbitrary units. *P<0.001. Control reactions performed with veins from *Pai1*$^{-/-}$ mice revealed no detectable PAI-1 gene expression (data not shown).

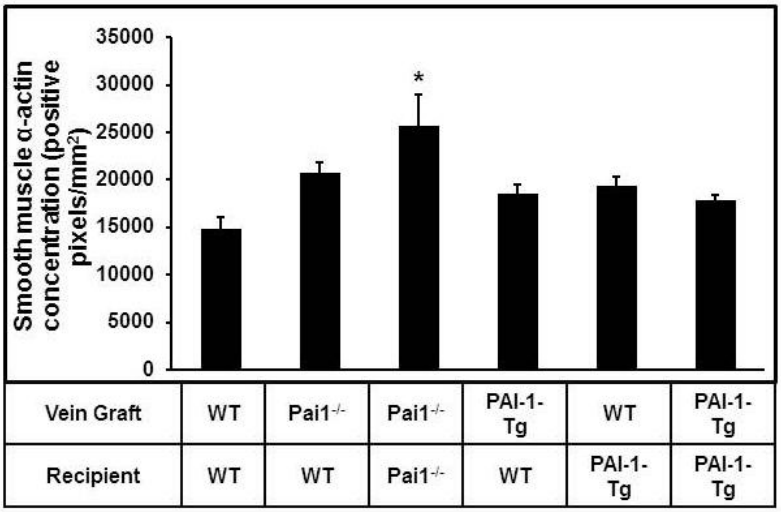

Supplemental Fig. III. Smooth muscle cell density in vein graft neointima, assessed by quantitative analysis of smooth-muscle-alpha-actin-positive pixels/mm^2. All groups consisted of 5 vein grafts. *P<0.05 vs. all other groups.

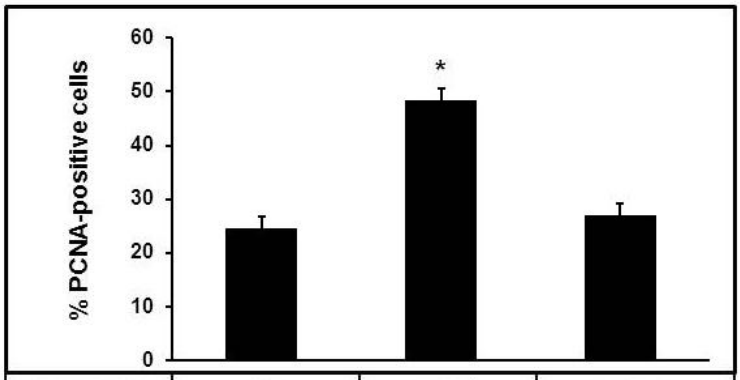

Vein Graft	WT	Pai1$^{-/-}$	PAI-1-Tg
Recipient	WT	Pai1$^{-/-}$	PAI-1-Tg
n	6	5	6

Supplemental Fig. IV. Rates of cell proliferation, assessed by anti-PCNA staining.

*P<0.05 vs. other groups.

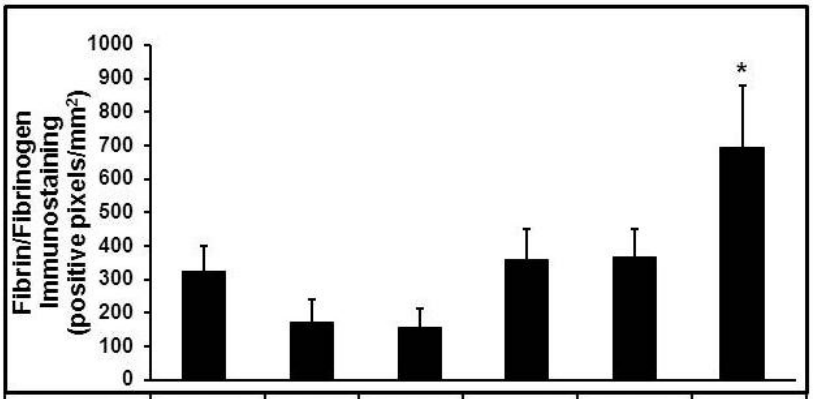

Vein Graft	WT	Pai1$^{-/-}$	Pai1$^{-/-}$	PAI-1-Tg	WT	PAI-1-Tg
Recipient	WT	WT	Pai1$^{-/-}$	WT	PAI-1-Tg	PAI-1-Tg
n	9	6	7	6	7	5

Supplemental Fig. V. Fibrin/fibrinogen immunostaining in vein graft neointima is increased in PAI-1-Tg^{graft}/PAI-1-Tg^{recipient} mice. *P<0.05 vs. *Pai1*$^{-/-graft}$/*Pai1*$^{-/-recipient}$, *Pai1*$^{-/-graft}$/WT^{recipient}, and WT^{graft}/WT^{recipient} mice.

References for Supplemental Methods and Figure Legends

(1) Carmeliet P, Kieckens L, Schoonjans L, Ream B, Nuffelen A, Prendergast G, Cole M, Bronson R, Collen D, Mulligan R. Plasminogen activator inhibitor-1 gene deficient mice. I. Generation by homologous recombination and characterization. *J Clin Invest* 1993;92:2746-55.

(2) Zheng X, Saunders T, Camper S, Samuelson L, Ginsburg D. Vitronectin is not essential for normal mammalian development and fertility. *Proc Natl Acad Sci* 1995;92:12426-30.

(3) Eitzman DT, McCoy RD, Zheng X, Fay WP, Shen T, Ginsburg D, Simon RH. Bleomycin-induced pulmonary fibrosis in transgenic mice that either lack or overexpress the murine plasminogen activator inhibitor-1 gene. *J Clin Invest* 1996;97:232-7.

(4) Shepherd CT, Moran Lauter AN, Scott MP. Determination of transgene copy number by real-time quantitative PCR. *Methods Molec Biol* 2009;526:129-34.

(5) Shitara H, Sato A, Hayashi Ji, Mizushima N, Yonekawa H, Taya C. Simple Method of Zygosity Identification in Transgenic Mice by Real-time Quantitative PCR. *Transgen Res* 2004;13:191-4.

(6) Salzberg SP, Filsoufi F, Anyanwu A, von Harbou K, Karlof E, Carpentier A, Dansky HM, Adams DH. Increased Neointimal Formation After Surgical Vein Grafting in a Murine Model of Type 2 Diabetes. *Circulation* 2006;114:I-302-I-307.

(7) Fickert P, Thueringer A, Moustafa T, Silbert D, Gumhold J, Tsybrovskyy O, Lebofsky M, Jaeschke H, Denk H, Trauner M. The role of osteopontin and tumor necrosis factor alpha receptor-1 in xenobiotic-induced cholangitis and biliary fibrosis in mice. *Lab Invest* 2010;90:844-52.

(8) Torzewski M, Ochsenhirt V, Kleschyov AL, Oelze M, Daiber A, Li H, Rossmann H, Tsimikas S, Reifenberg K, Cheng F, Lehr HA, Blankenberg S, Forstermann U, Munzel T, Lackner KJ. Deficiency of Glutathione Peroxidase-1 Accelerates the Progression of Atherosclerosis in Apolipoprotein E-Deficient Mice. *Arterioscler Thromb Vasc Biol* 2007;27:850-7.

(9) Livak KJ, Schmittgen TD. Analysis of Relative Gene Expression Data Using Real-Time Quantitative PCR and the 2-[Delta][Delta]CT Method. *Methods* 2001;25:402-8.

(10) Ray JL, Leach R, Herbert J-M, Benson M. Isolation of vascular smooth muscle cells from a single murine aorta. *Meth Cell Sci* 2002;23:185-8.

(11) Garg N, Goyal N, Strawn TL, Wu J, Mann KM, Lawrence DA, Fay WP. Plasminogen activator inhibitor-1 and vitronectin expression level and stoichiometry regulate vascular smooth muscle cell migration through physiological collagen matrices. *J Thromb Haemost* 2010;8:1847-54.

(12) Suh TT, Holmback K, Jensen NJ, Daugherty CC, Small K, Simon DI, Potter S, Degen JL. Resolution of spontaneous bleeding events but failure of pregnancy in fibrinogen-deficient mice. *Genes Dev* 1995;9:2020-33.

(13) Bezerra JA, Currier AR, Melin-Aldana H, Sabla G, Bugge TH, Kombrinck KW, Degen JL. Plasminogen Activators Direct Reorganization of the Liver Lobule after Acute Injury. *Am J Pathol* 2001;158:921-9.